International Journal of Pharmaceutics 368 (2009) 89–97

Contents lists available at ScienceDirect

International Journal of Pharmaceutics

journal homepage: www.elsevier.com/locate/ijpharm

In vitro and *in vivo* evaluation of a paclitaxel conjugate with the divalent peptide E-[c(RGDfK)$_2$] that targets integrin $\alpha_v\beta_3$

Claudia Ryppa[a], Hagit Mann-Steinberg[b], Martin L. Biniossek[c], Ronit Satchi-Fainaro[b,*], Felix Kratz[a,1]

[a] Tumor Biology Center, Breisacher Straße 117, 79106 Freiburg, Federal Republic of Germany
[b] Department of Physiology and Pharmacology, Sackler School of Medicine, Tel-Aviv University, Tel-Aviv 69978, Israel
[c] Institut für Molekulare Medizin und Zellforschung, Zentrum für Biochemie und Molekulare Zellforschung, Stefan-Meier-Straße 17, 79104 Freiburg, Federal Republic of Germany

ARTICLE INFO

Article history:
Received 13 August 2008
Received in revised form
29 September 2008
Accepted 30 September 2008
Available online 17 October 2008

Keywords:
Integrins
RGD peptides
Paclitaxel
Prodrugs
Vascular targeting

ABSTRACT

The $\alpha_v\beta_3$ integrin is overexpressed on proliferating endothelial cells such as those present in growing tumors as well as on tumor cells of various origins. Tumor-induced angiogenesis can be inhibited *in vivo* by antagonizing the $\alpha_v\beta_3$ integrin with small peptides containing the arginyl-glycyl-aspartic acid (RGD) amino acid sequence. The divalent cyclic peptide E-[c(RGDfK)$_2$] is a novel ligand-based vascular-targeting agent that binds integrin $\alpha_v\beta_3$ and demonstrated high uptake in OVCAR-3 xenograft tumors. In this work, we coupled the 2′-OH-group of paclitaxel through an aliphatic ester to the amino group of E-[c(RGDfK)$_2$] or the control peptide c(RADfK), thus obtaining the derivatives E-[c(RGDfK)$_2$]-paclitaxel and c(RADfK)-paclitaxel. Subsequently, we investigated the activity of the paclitaxel derivatives using several well-established *in vitro* angiogenesis assays: using a standard 72 h endothelial cell proliferation assay, we showed that both E-[c(RGDfK)$_2$]-paclitaxel and c(RADfK)-paclitaxel inhibit the proliferation of human umbilical vein endothelial cells (HUVEC) in a similar manner as free paclitaxel (IC_{50} value ~0.4 nM), an observation that can be explained by the half-life of the paclitaxel ester bond in the conjugates of ~2 h at pH 7. In contrast, a 30-min exposure of the cells to the three drugs showed a clear difference between free paclitaxel, E-[c(RGDfK)$_2$]-paclitaxel and c(RADfK)-paclitaxel with IC_{50} values of 10 nM, 25 nM, and 60 nM, respectively. These differences are very likely due to the different routes of cellular entry of these three molecules. While the hydrophobic paclitaxel diffuses rapidly through the cell membrane, the charged peptide-containing derivative E-[c(RGDfK)$_2$]-paclitaxel binds to the overexpressed $\alpha_v\beta_3$ integrin in order to enter the cells via receptor-mediated endocytosis. The differences between the derivatives were further demonstrated using an endothelial cell adhesion assay. Inhibition of cell attachment was observed only with the E-[c(RGDfK)$_2$]-paclitaxel derivative indicating its specificity to the growing endothelial cells. Furthermore, E-[c(RGDfK)$_2$]-paclitaxel inhibited both endothelial cells migration and capillary-like tube formation. These results further demonstrate their antiangiogenic properties. *In vivo* studies in an OVCAR-3 xenograft model demonstrated no antitumor efficacy for either E-[c(RGDfK)$_2$] or E-[c(RGDfK)$_2$]-paclitaxel compared to moderate efficacy for paclitaxel.

© 2008 Elsevier B.V. All rights reserved.

1. Introduction

Integrins have been intensely studied as endothelial targets for antiangiogenic therapy and for vascular targeting strategies (Temming et al., 2005; Tucker, 2006). Integrins are heterodimeric cell surface receptors of which several such as integrin $\alpha_v\beta_3$, $\alpha_v\beta_5$, and $\alpha_5\beta_1$ are overexpressed in the blood vessels of solid tumors and mediate adhesion between cells and the extracellular matrix thus promoting tumor cell migration and tumor growth. A characteristic feature of integrins is their high binding affinity for arginyl-glycyl-aspartic acid (RGD) sequences exposed on endogenous or exogenous ligands. Kessler and colleagues have developed a series of cyclic RGD peptides that interact with integrin $\alpha_v\beta_3$ and $\alpha_v\beta_5$ (Aumailley et al., 1991; Dechantsreiter et al., 1999; Haubner et al., 1996; Pfaff et al., 1994). One of these, cyclo(RGDfV) (Cilengitide), was chosen as a clinical candidate after demonstrating antiangiogenic and antitumor efficacy in preclinical tumor models (Buerkle

* Corresponding author at: Department of Physiology and Pharmacology Sackler School of Medicine Tel Aviv University, Tel Aviv 69978, Israel. Tel.: +972 3 640 7427; fax: +972 3 640 9113.
E-mail addresses: ronitsf@post.tau.ac.il (R. Satchi-Fainaro), felix@tumorbio.uni-freiburg.de (F. Kratz).
[1] Tumor Biology Center, Department of Medical Oncology, Clinical Research, Breisacher Straße 117, D-79106 Freiburg, Federal Republic of Germany.
Tel.: +49 761 2062930; fax: +49 761 2062905.

0378-5173/$ – see front matter © 2008 Elsevier B.V. All rights reserved.
doi:10.1016/j.ijpharm.2008.09.055

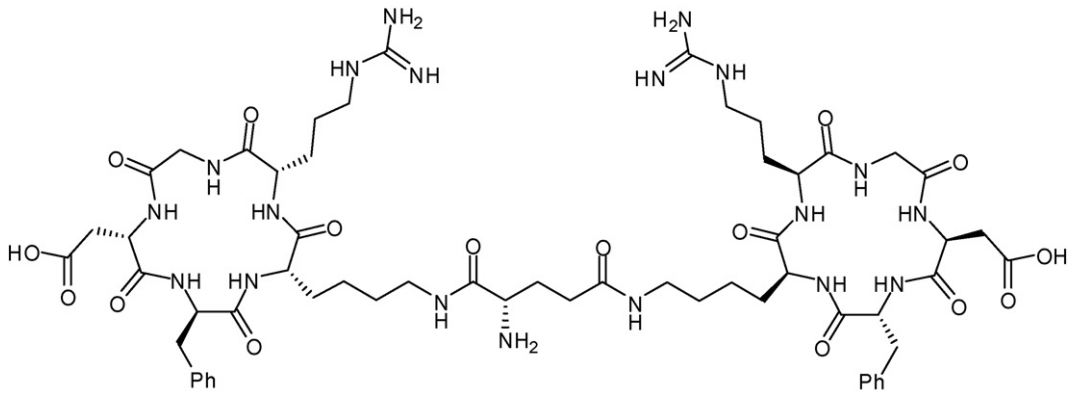

Fig. 1. Structure of E-[c(RGDfK)$_2$].

et al., 2002; MacDonald et al., 2001). In clinical trials, Cilengitide has shown antitumor efficacy against glioblastoma (Friess et al., 2006; Nabors et al., 2007), but no improvement in treating pancreas carcinoma in combination with gemcitabin compared to gemcitabin alone (Friess et al., 2006). A number of phase II trials are currently ongoing.

A potential disadvantage of integrin $\alpha_v\beta_3$ antagonists is their insufficient anti-proliferative effect on endothelial cells and their poor bioavailability necessitating fairly large doses for human use due to a short half-life of only a few hours. Vascular targeting agents that consist of a targeting moiety and an effector molecule are a possibility of improving the therapeutic efficacy of integrin $\alpha_v\beta_3$ binding ligands. For this purpose a stable peptide derivative c(RGDfK) based on the structure of Cilengitide has been developed that shows specific tumor targeting properties (Janssen et al., 2002a,b, 2004). The presence of the glutamic acid residue makes it an ideal ligand for further chemical conjugation with diagnostic or therapeutic agents. In further diagnostic studies, Janssen et al. demonstrated that a dimeric form of c(RGDfK) (Fig. 1), i.e. E-[c(RGDfK)$_2$], had improved tumor targeting properties over the monomeric form (Janssen et al., 2002b; Burkhart et al., 2004). Subsequent biodistribution studies with radiolabeled E-[c(RGDfK)$_2$] showed an uptake of up to 7.5% injected dose/g in OVCAR-3 xenograft tumors (Janssen et al., 2002b).

A tyrosine derivative of E-[c(RGDfK)$_2$], i.e. E-[c(RGDyK)$_2$], that can be conveniently radiolabeled with ^{125}I, was used for developing a E-[c(RGDyK)$_2$]-paclitaxel derivative in which paclitaxel was bound at the 2′-OH-position through a succinate spacer to the α-amino position of the glutamic acid residue of E-[c(RGDyK)$_2$] (Chen et al., 2005). This conjugate showed integrin $\alpha_v\beta_3$ binding, a threefold higher IC$_{50}$ value in a 48-h assay against MDA-MB-435 breast cancer cells and a maximum tumor uptake of the radiolabeled E-[c(RGDyK)$_2$]-paclitaxel derivative 2 h post-injection (~2.7% ID/g) in the MDA-MB-435 xenograft model, a value comparable to radiolabeled E-[c(RGDyK)$_2$] (~2.4% ID/g) run as control in this experiment. No stability was reported for the ester bond, but premature release of paclitaxel was mentioned by Temming et al. when using the succinate ester of paclitaxel for their development of RGD-paclitaxel albumin conjugates (Temming et al., 2005). *In vivo* data of the E-[c(RGDyK)$_2$]-paclitaxel conjugate showing an antitumor effect were recently published (Cao et al., 2008).

As part of our ongoing projects on passive and active targeting with prodrugs (Kratz et al., 2008), we wanted to examine, in more detail, the *in vitro* properties of the paclitaxel succinate ester derivative with E-[c(RGDfK)$_2$] and the control peptide c(RADfK) that does not bind to integrin $\alpha_v\beta_3$. In this work, we report on their cytotoxicity in short- and long-term incubation experiments with human umbilical vein endothelial cells (HUVEC) as well as on their activity in a cell adhesion, migration, and capillary-like tube formation assay. Additional *in vivo* results in an OVCAR-3 xenograft model are presented.

2. Materials and methods

2.1. Materials, methods, and spectroscopy

Paclitaxel was purchased from Yick-Vic (Hong Kong, PRC); E-[c(RGDfK)$_2$] and c(RADfK) were purchased from Peptides International (Louisville, KY, USA); organic solvents: HPLC grade (Labscan Ltd., Dublin, Ireland; Roth, Karlsruhe, FRG; Merck, Darmstadt, FRG). The aliphatic paclitaxel-NHS-ester was prepared by a modified procedure according to the literature (Deutsch et al., 1989; Luo and Prestwich, 1999). All other chemicals used were at least reagent grade and obtained from Sigma–Aldrich (Deisenhofen, FRG) or Merck and used without further purification; buffers were vacuum-filtered through a 0.2-μm membrane (Sartorius, FRG) and thoroughly degassed with nitrogen prior to use. ^{1}H, ^{13}C NMR: Bruker AM 400 (internal standard: TMS); analytical HPLC and the stability study were performed with a Kontron 422 pump and a Kontron 430 detector (at 220 nm). For peak integration Geminyx software (version 1.91 by Goebel Instrumentelle Analytik, FRG) was used; column: Machery-Nagel, 100 Å, Nucleosil 100-5 C18 [4 mm × 250 mm] with pre-column WAT106166; chromatographic conditions for the analytical HPLC: flow: 1.0 mL/min, mobile phase A: AcN/0.05% aqu. TFA (30/70, v/v), mobile phase B: AcN/0.05% aqu. TFA (70/30, v/v), gradient: 0–1.5 min 100% mobile phase A; 1.5–40 min increase to mobile phase B; 40–46.5 min decrease to initial mobile phase A; injection volume: 20 μL. Chromatographic conditions for the stability study: flow: 1.0 mL/min, mobile phase A: AcN/0.05% aqu. TFA (5/95, v/v), mobile phase B: AcN/0.05% aqu. TFA (70/30, v/v), gradient and injection volume: as described above. Lyophilization was performed overnight at −40 °C with a Christ Alpha 2–4 (Gefriertrocknungs GmbH, FRG) lyophilizer. MALDI-TOF mass spectra were acquired on a Reflex III mass spectrometer (Bruker Daltonik GmbH, Bremen, FRG) in the reflector mode (positively charged ions) with external calibration. Samples were prepared with an adapted thin-layer technique (Kussmann et al., 1997). α-Cyano-4-hydroxycinnamic acid (97%, Aldrich, Taufkirchen, FRG) was used as matrix and nitrocellulose (Biorad, München, FRG, Trans-Blot Transfer Medium) as additive. The samples were washed with 0.1% TFA. Monoisotopic peaks were used for data analysis. ESI-TOF mass spectra were acquired on an Agilent 6210 system, consisting of an Agilent 1100 HPLC system with a diode array detector and an ESI-MSD TOF by Agilent Technologies (Böblingen, FRG).

2.2. Synthesis of the aliphatic paclitaxel-NHS-ester

To a solution of paclitaxel (600 mg, 0.703 mmol, 1 equiv.) and succinic anhydride (91 mg, 0.913 mmol, 1.3 equiv.) in dry DCM (10 mL) was added a solution of DMAP (111 mg, 0.913 mmol, 1.3 equiv.) in DCM (5 mL). The mixture was stirred at room temperature overnight, the solvent was evaporated *in vacuo* and the residue was purified by column chromatography on silica gel with ethyl acetate/MeOH (5/1, v/v) to obtain the paclitaxel-hemisuccinate as a white powder in 80% yield (540 mg, 0.565 mmol). Analytic data (^{1}H NMR, MS) were in accord with the literature (Dosio et al., 1997). To a solution of the paclitaxel-hemisuccinate (463 mg, 0.485 mmol, 1.1 equiv.) and DCC (91 mg, 0.443 mmol, 1.1 equiv.) in dry THF (3 mL) *N*-hydroxysuccinimide (51 mg, 0.443 mmol, 1 equiv.) was added and the mixture was stirred at room temperature overnight. The mixture was precipitated in Et_2O (20 mL), washed with Et_2O (2 × 5 mL) and dried *in vacuo*. The residue was purified by column chromatography on diol with ethyl acetate/*n*-hexane (2/1, v/v) to obtain the paclitaxel-NHS ester as a white powder in 43% yield (220 mg, 0.209 mmol). Analytic data (MS) were in accord with the literature (Luo and Prestwich, 1999).

2.3. Synthesis of E-[c(RGDfK)$_2$]-paclitaxel and c(RADfK)-paclitaxel

2.3.1. E-[c(RGDfK)$_2$]-paclitaxel

The aliphatic paclitaxel-NHS-ester (100 mg, 95.0 μmol, 1.1 equiv.) and E-[c(RGDfK)$_2$] (114 mg, 86.5 μmol, 1 equiv.) were dissolved in DMF (4.5 mL) containing DIEA (29 μL, 173 μmol, 2 equiv.) and H_2O (10%, v/v). The mixture was kept overnight at room temperature. The solvent was reduced *in vacuo*, the residue was precipitated in Et_2O (120 mL), washed with Et_2O, DCM, and THF (10 mL), filtered and dried *in vacuo*. The compound was lyophilized at −30 °C at a concentration of 1 mg/mL from AcN/0.1N HCl (1/1, v/v) to obtain a white powder in 59% yield (119 mg, 51 μmol). HPLC purity: 26.8 min, 97% of peak area, 220 nm; MS (TOF) m/z = 2275.96 $[M+Na]^+$, 2253.98 $[M+H]^+$, 1440.63 $[C_{63}H_{91}N_{19}O_{19}Na]^+$, 1418.66 $[C_{63}H_{92}N_{19}O_{19}]^+$, 1400.64 $[C_{63}H_{90}N_{19}O_{18}]^+$, 1318.64 $[C_{59}H_{88}N_{19}O_{16}]^+$.

2.3.2. c(RADfK)-paclitaxel

The aliphatic paclitaxel-NHS-ester (100 mg, 95.0 μmol, 1.1 equiv.) and c(RADfK) (53 mg, 86.5 μmol, 1 equiv.) were dissolved in DMF (2 mL) containing DIEA (29 μL, 173 μmol, 2 equiv.). The mixture was kept overnight at room temperature. The solvent was reduced *in vacuo*, the residue was precipitated in Et_2O (120 mL), washed with Et_2O (2 × 20 mL) and H_2O (3 × 50 mL), filtered and dried *in vacuo*. The compound was lyophilized at −30 °C at a concentration of 1 mg/mL from AcN/0.1N HCl (1/1, v/v) to obtain a white powder in 79% yield (108 mg, 68 μmol). HPLC purity: 29.1 min, 89% of peak area, 220 nm; MS (TOF) m/z = 2275.02 $[C_{111}H_{141}N_{19}O_{32}+Na]^+$ (diesterified byproduct), 2253.05 $[C_{111}H_{141}N_{19}O_{32}+H]^+$, 1750.74 $[C_{87}H_{104}N_{11}O_{28}]^+$, 1575.60 $[M+Na]^+$, 1553.67 $[M+H]^+$ (base peak), 985.52 $[C_{48}H_{61}N_{10}O_{13}]^+$.

2.4. Stability study of E-[c(RGDfK)$_2$]-paclitaxel

A 200 μM solution of E-[c(RGDfK)$_2$]-paclitaxel in glucose phosphate buffer (10 mM sodium phosphate, 5% D-(+)-glucose, pH 7, containing 2.5% DMSO) was prepared and incubated at 37 °C. Samples were collected and analyzed by HPLC over 24 h using the HPLC method described under Section 2.1 (see above).

2.5. Endothelial cell proliferation assay

HUVEC were plated onto 24-well plates (1.5 × 10^4 cells/well) in EBM-2 medium (Clonetics, Walkersville, MD, USA) supplemented with 5% FBS and incubated for 24 h (37 °C; 5% CO_2). On the following day, the cultured medium was removed and cells were exposed to serial dilutions of paclitaxel and paclitaxel derivatives prepared in a fresh mixture of EBM-2 medium and EGM-2 complete medium (Clonetics) (1:1, v/v). Cell proliferation was assessed after 72 h by means of direct counting using a Z1 Coulter® Particle Counter (Beckman Coulter™, Miami, FL, USA). As positive control, cells were grown without treatment, as negative control cells were grown in EBM-2 medium supplemented with 5% FBS. Each treatment was assayed in triplicates and the experiment was repeated independently. Proliferation of endothelial cells was normalized to percent cell growth compared to the cell growth of the positive untreated control cells. Error bars represent the standard deviation of the mean.

2.6. Endothelial cell proliferation assay–short exposure variation

This assay was performed as the standard one described above with the exception that the cells were exposed to the drugs for a shorter period of time. After the indicated times, cells were washed with EBM-2 serum free medium (Clonetics) and then were incubated for the rest of the 72 h with a fresh mixture of EBM-2 medium and EGM-2 complete medium (Clonetics) (1:1, v/v) without additional treatment.

2.7. Endothelial cell migration assay

Cell migration assay was performed using modified 8 μm Boyden chambers (Transwell-Costar Corp., Cambridge, MA, USA) coated with 10 μg/mL fibronectin. HUVEC were challenged with paclitaxel and the paclitaxel derivatives at serial concentrations and were added to the upper chamber of the transwell (5 × 10^4 cells/chamber) for 2 h. After incubation, the cells were allowed to migrate towards vascular endothelial growth factor (VEGF) (20 ng/mL) to the underside of the chamber for 4 h. Cells were fixed and stained (Hema 3 Stain System; Fisher Diagnostics, Houston, TX, USA). The number of migrated cells per membrane was captured using bright-field microscopy connected to a spot digital camera (Diagnostic Instruments, Sterling Heights, MI, USA). Migrated cells from the captured image were counted using NIH ImageJ processing and analysis software. Each determination represents the average of three individual wells, and error bars represent the standard deviation (S.D.). Migration of endothelial cells was normalized to percent migration, with migration to VEGF alone representing 100% migration.

2.8. Endothelial cell capillary-like tube formation assay

The surface of 24-well plates was coated with cultrex® basement membrane (50 μL/well; 10 mg/mL) on ice and was then allowed to polymerize at 37 °C for 30 min. HUVEC (3 × 10^4) were challenged with paclitaxel and paclitaxel derivatives and then were seeded on coated plates in the presence of complete EGM-2 medium. After 8 h of incubation (37 °C; 5% CO_2), wells were imaged using Nikon TE2000E inverted microscope integrated with Nikon DS5 cooled CCD camera by 4X objective, brightfield technique. Tubes from the captured image were counted using NIH ImageJ processing and analysis software.

2.9. Endothelial cell adhesion assay

The bioactivity of the E-[c(RGDfK)$_2$] peptide after the conjugation to paclitaxel was assessed using an adhesion assay. Flat bottom 96-well culture plates (Nunc, Roskilde, Denmark) were coated with 0.5 μg/well fibrinogen (Sigma–Aldrich) overnight at 4 °C. After washing three times with PBS, the wells were blocked with 1% bovine serum albumin (BSA) for 1 h at 37 °C and washed three times again with PBS. HUVEC were harvested in phosphate-buffered saline (137 mM NaCl, 2.7 mM KCl, 4.3 mM Na_2HPO_4, 1.4 mM KH_2PO_4, pH 7.3) with 2.5 mM EDTA and resuspended in EBM-2 serum-free media (Clonetics). In separate experiments HUVEC were incubated (30 min, at room temperature) with either paclitaxel, paclitaxel derivatives, E-[c(RGDfK)$_2$] or c(RADfK) as controls. The treated HUVEC were plated at 5×10^4 cells/well and were allowed to attach for 1 h at 37 °C. After incubation, the unattached cells were removed by rinsing the wells with PBS. The attached cells were fixed with 3.7% formaldehyde, stained with 0.5% crystal violet and were imaged using Nikon TE2000E inverted microscope integrated with Nikon DS5 cooled CCD camera by 4× objective, brightfield technique. The number of attached cells was quantified with NIH ImageJ processing and analysis software.

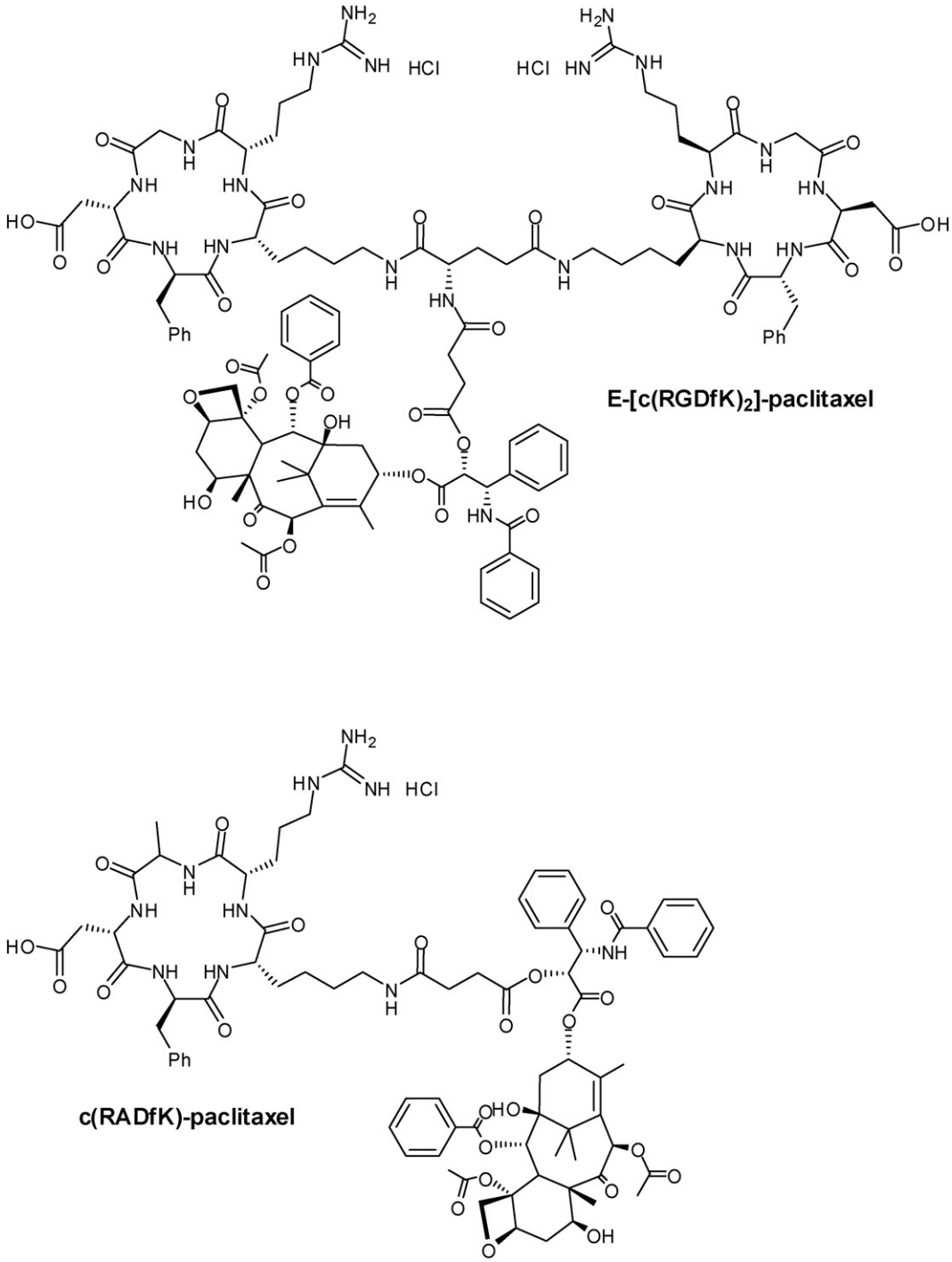

Fig. 2. Structure of E-[c(RGDfK)$_2$]-paclitaxel and c(RADfK)-paclitaxel.

Non-specific binding was determined by adhesion to BSA-coated plates.

2.10. In vivo experiments

For the *in vivo* testing of E-[c(RGDfK)$_2$] and E-[c(RGDfK)$_2$]-paclitaxel in comparison with paclitaxel female NMRI: nu/nu mice (M&B A/S, Ry, Denmark) were used. The mice were held in laminar flow shelves under sterile and standardized environmental conditions (25 ± 2 °C room temperature, 50 ± 10% relative humidity, 12 h light–dark-rhythm). They received autoclaved food and bedding (ssniff, Soest, FRG) and acidified (pH 4.0) drinking water *ad libitum*. All animal experiments were performed under the auspices of the German Animal Protection Law. For experiments in tumor-bearing animals, 10^7 cells of human ovarian cancer cells OVCAR-3 from *in vitro* culture were transplanted subcutaneously (s.c.) into the flank region of anaesthetized (40 mg/kg i.p. Radenarkon, Asta Medica, Frankfurt, FRG) mice on day zero. Mice were randomly distributed to the experimental groups (eight mice each for control, E-[c(RGDfK)$_2$]-paclitaxel, and paclitaxel, six mice for E-[c(RGDfK)$_2$]). When the tumors were grown to a palpable size, treatment was initiated (Fig. 8). Mice were treated intravenously at day 10, 17, and 24 with either glucose phosphate buffer (10 mM sodium phosphate, 5% D-(+)-glucose, pH 5.8), E-[c(RGDfK)$_2$], dissolved in glucose phosphate buffer (10 mM sodium phosphate, 5%

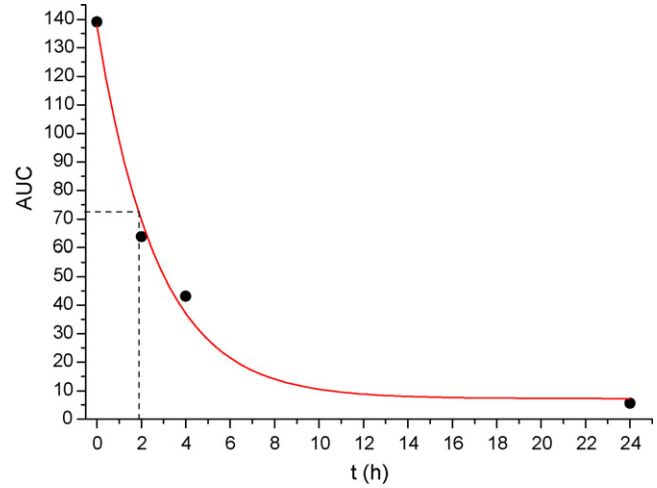

Fig. 3. Stability study of a 200-μM solution of E-[c(RGDfK)$_2$]-paclitaxel at pH 7 at 37 °C. Plotted is the decrease of the peak area of E-[c(RGDfK)$_2$]-paclitaxel at 220 nm. Chromatographic conditions: see Section 2.1.

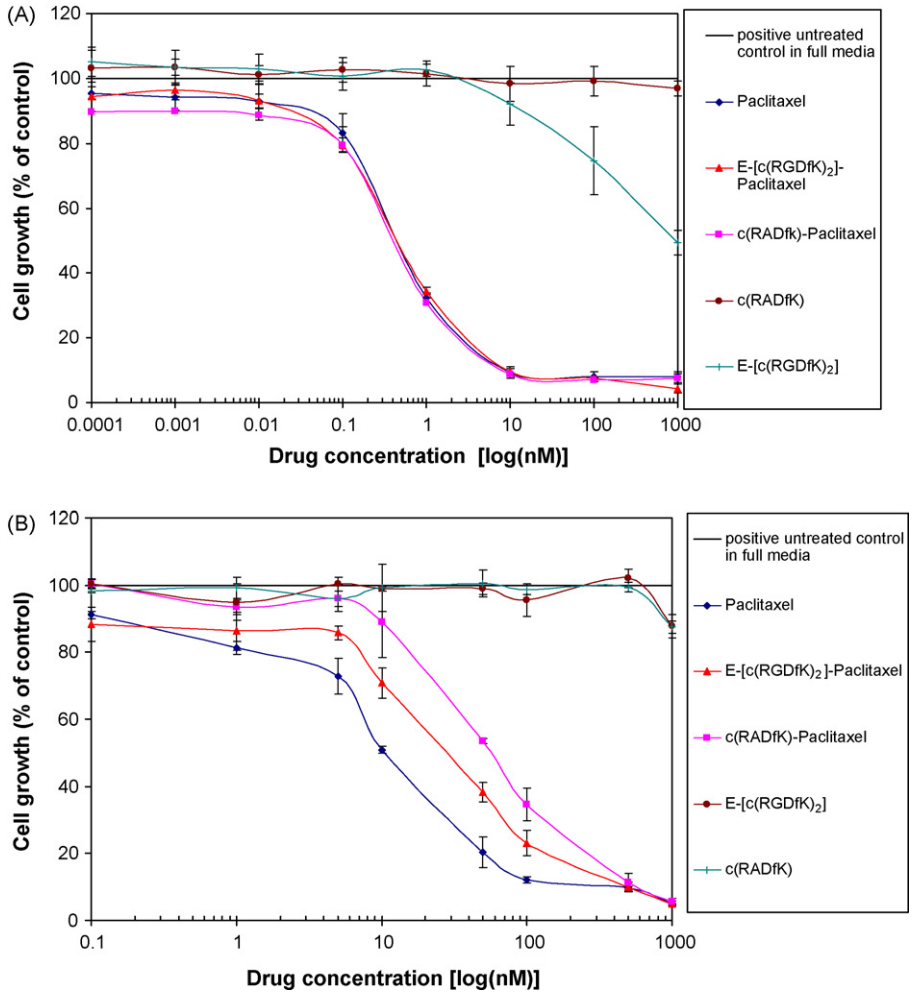

Fig. 4. Endothelial cell proliferation assay with paclitaxel, the paclitaxel derivatives, E-[c(RGDfK)$_2$] and c(RADfK): (A) a standard 72 h proliferation assay demonstrates that free paclitaxel, E-[c(RGDfK)$_2$]-paclitaxel and c(RADfK)-paclitaxel inhibited HUVEC proliferation at a similar manner. (B) a 30 min exposure proliferation assay on HUVEC demonstrates the differences between the three derivatives.

D-(+)-glucose, pH 5.8) at a concentration of 7 mM (3 × 54.5 mg/kg), paclitaxel (2 × 12 mg/kg), and E-[c(RGDfK)$_2$]-paclitaxel, dissolved in glucose phosphate buffer (10 mM sodium phosphate, 5% D-(+)-glucose, pH 5.8) at a concentration of 180 μM (3 × 12 mg/kg).

Tumor size was measured twice weekly with a caliper-like instrument in two dimensions. Individual tumor volumes (V) were calculated by the formula $V = (\text{length} \times [\text{width}]^2)/2$ and related to the values on the first day of treatment (relative tumor volume, RTV). Statistical analysis was performed with the U-test (Mann and Whitney) with $p < 0.05$. The body weight of mice was determined every 3–4 days.

3. Results and discussion

The hemisuccinate derivative of paclitaxel was prepared by esterification of the 2′-hydroxy function of paclitaxel with succinic anhydride according to a modified procedure of Deutsch et al. (1989). Subsequent activation with NHS and DCC according to a modified procedure by Luo and Prestwich (1999) and coupling to the cyclic peptides E-[c(RGDfK)$_2$] or c(RADfK) followed by lyophilization resulted in the HCl salts of E-[c(RGDfK)$_2$]-paclitaxel in 59% yield and c(RADfK)-paclitaxel in 79% yield (Fig. 2). E-[c(RGDfK)$_2$]-paclitaxel showed good water-solubility in glucose phosphate buffer (10 mM sodium phosphate, 5% D-(+)-glucose, pH 5.8) of ∼10 mg/mL, while conjugate c(RADfK)-paclitaxel was soluble at 500 μM in 0.1 M HCl containing 5% DMSO. The purity of the conjugates was determined by analytical HPLC and molecular mass using MALDI-TOF (see Section 2).

The stability of E-[c(RGDfK)$_2$]-paclitaxel was studied at pH 7 by HPLC over 24 h yielding a half-life of ∼2 h at 37 °C (Fig. 3) and demonstrating a release of paclitaxel.

In order to assess the antiangiogenic properties of the paclitaxel derivatives, we first tested their ability to inhibit HUVEC proliferation using a standard 72 h proliferation assay. Here we show that both E-[c(RGDfK)$_2$]-paclitaxel and c(RADfK)-paclitaxel inhibited the proliferation of HUVEC in a similar manner as the free paclitaxel at paclitaxel-equivalent concentrations ranging from 0.1 pM to 1 μM providing an IC_{50} of 0.4 nM (Fig. 4A). The free peptides c(RADfK) and E-[c(RGDfK)$_2$] served as controls. The E-[c(RGDfK)$_2$] peptide by itself inhibited the proliferation of endothelial cells at high concentrations of 100–1000 nM while the c(RADfK) peptide showed no effect even at these concentrations. The reason for the lack of any difference in cytotoxicity between the paclitaxel ester derivatives and the free drug over 72 h is the limited stability of the ester bond under neutral conditions. We therefore examined whether a short exposure of the cells to the aliphatic paclitaxel derivatives would demonstrate difference in activity. We show that a 30-min incubation of the cells with the drugs (30 min pulse) changes the proliferation growth curves in a manner that demonstrates the differences between the free paclitaxel, E-[c(RGDfK)$_2$]-paclitaxel and c(RADfK)-paclitaxel with IC_{50} values of 10 nM, 25 nM, and 60 nM, respectively (Fig. 4B). Other short time exposures of the cells to the drugs were also tested (IC_{50} values are summarized in Table 1) and demonstrating a difference between the activity of E-[c(RGDfK)$_2$]-paclitaxel and c(RADfK)-paclitaxel.

Table 1
IC_{50} values of paclitaxel and paclitaxel derivatives in differently designed proliferation experiments.

Duration of Pulse	Paclitaxel	E-[c(RGDfK)$_2$]-paclitaxel	c(RADfK)-paclitaxel
72 h	0.4 nM	0.4 nM	0.4 nM
60 min	6 nM	30 nM	90 nM
45 min	10 nM	25 nM	100 nM
30 min	10 nM	25 nM	60 nM
20 min	8 nM	20 nM	60 nM

Two further assays were chosen in order to demonstrate that the conjugation of paclitaxel to the peptides c(RADfK) or E-[c(RGDfK)$_2$] did not affect the antiangiogenic properties of paclitaxel: The migration assay and capillary-like tube formation assay that evaluate the drugs' effect on two steps in the angiogenic cascade necessary for vessel recruitment and tumor development.

First, we examined the effect of the paclitaxel derivatives on VEGF-induced endothelial cell migration. Migration was assessed by counting the number of cells that migrated through the membranes towards VEGF during a 4-h period following 2 h pre-treatment with 0.4 nM of either free paclitaxel, E-[c(RGDfK)$_2$]-paclitaxel or c(RADfK)-paclitaxel as control. Treatment with all three aliphatic derivatives inhibited the chemotactic migration response to VEGF by ∼40% (Fig. 5). The second antiangiogenic assay that was chosen in order to test the activity of the paclitaxel aliphatic derivatives was the capillary-like tube formation assay. Briefly, HUVEC were seeded on matrigel coated 24-well plates in the presence or absence of treatments with paclitaxel derivatives and were allowed to form tubular structures. Cells in the wells were imaged following 8 h of incubation. The results presented here demonstrate that 1 nM paclitaxel-equivalent concentration completely inhibited the formation of tubular structures of HUVEC while 0.1 nM inhibited endothelial tube formation by ∼45% (Fig. 6).

Finally, an endothelial cell adhesion assay was performed in order to evaluate *in vitro* the targeting specificity of the E-[c(RGDfK)$_2$]-containing paclitaxel derivative. Briefly, HUVEC were detached with 2.5 nM EDTA and resuspended in serum free medium at 5×10^5 cells/mL. Cells were incubated for 30 min in the presence or absence of the indicated treatments and were plated on fibrinogen-coated plates and allowed to attach. After incubation of

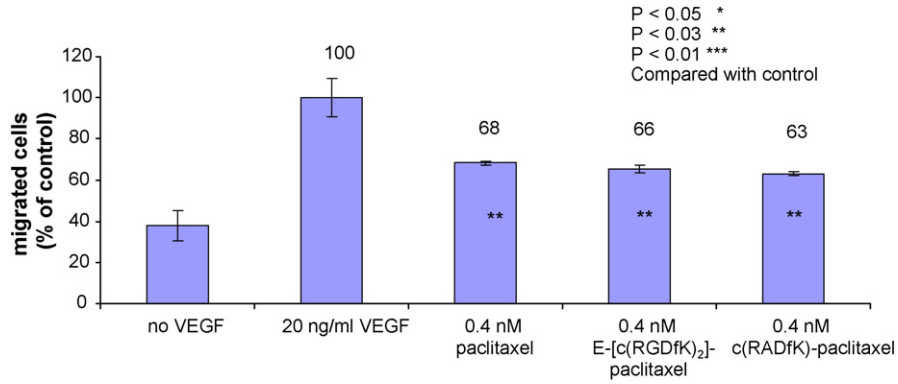

Fig. 5. Paclitaxel and paclitaxel derivatives inhibited HUVEC migration towards VEGF.

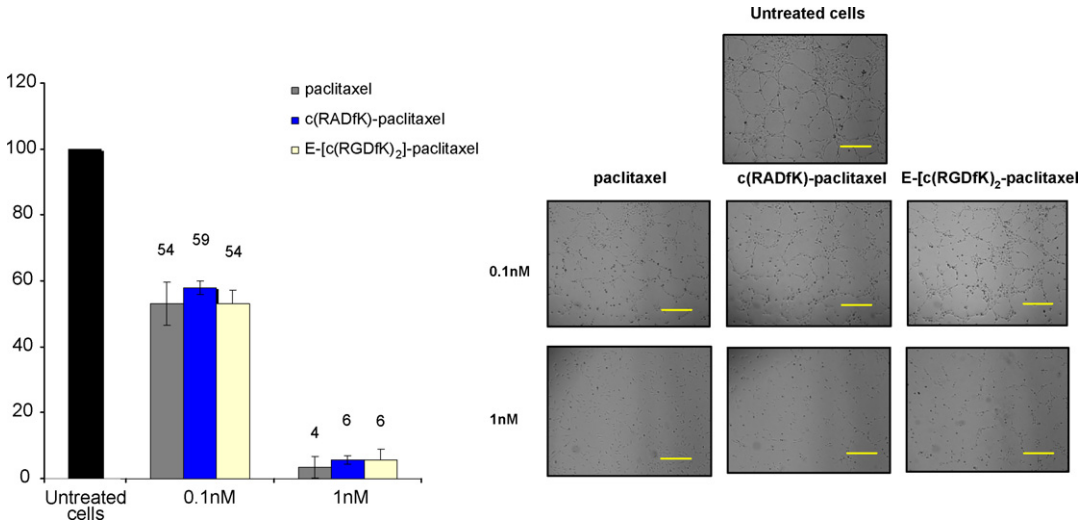

Fig. 6. Paclitaxel and paclitaxel derivatives inhibited HUVEC capillary-like tube formation dose-responsively.

1 h at 37 °C, unattached cells were removed and the adherent cells were fixed, stained with crystal violet and their number was determined. Our results demonstrate that E-[c(RGDfK)$_2$]-paclitaxel was able to inhibit HUVEC adhesion to fibrinogen in a dose dependent manner (Fig. 7). At 50 000 nM, E-[c(RGDfK)$_2$]-paclitaxel completely inhibited the adhesion of the cells to fibrinogen and at 500 nM, and 50 nM inhibition was 60% and 33%, respectively. At 5 nM, E-[c(RGDfK)$_2$]-paclitaxel no longer had an effect on endothelial cells adhesion. In both experiments, free paclitaxel itself inhibited the adhesion of the cells at 50,000 nM probably due to its direct toxicity to the cells (decreasing cell number). At all the other concentrations 500 nM, 50 nM, and 5 nM both free paclitaxel and c(RADfK)-paclitaxel had no significant effect on endothelial cell adhesion. The free peptides E-[c(RGDfK)$_2$] and c(RADfK) served as controls. As expected, the E-[c(RGDfK)$_2$] peptide completely abrogated HUVEC adhesion at 50,000 nM while at the same concentration the c(RADfK) peptide had no effect on the cells (Fig. 7A). In order to investigate whether the antiangiogenic effect of E-[c(RGDfK)$_2$]-paclitaxel was primarily due to the effect of the peptide E-[c(RGDfK)$_2$] or the conjugate itself, we repeated the cell adhesion experiment with various concentrations of E-[c(RGDfK)$_2$] as well as of c(RADfK) (200 nM to 200,000 nM). As shown in Fig. 7B, c(RADfK) is inactive at all concentrations whereas E-[c(RGDfK)$_2$] showed a clear dose-dependent response with ~99% inhibition at 200,000 nM, 80% inhibition at 20,000 nM, 36% inhibition at 2000 nM, and only 3% inhibition at 200 nM. When comparing the activity of the free peptide with that of the conjugate E-[c(RGDfK)$_2$]-paclitaxel, it is evident that the antiangiogenic effect of E-[c(RGDfK)$_2$]-paclitaxel is not solely due to the RGD peptide but also due to an uptake of paclitaxel into HUVEC cells because cell adhesion inhibition is 60% at a concentration of 500 nM which is significantly larger than that of the free RGD peptide at the higher concentration of 2000 nM (compare Fig. 7A and B).

Furthermore the *in vivo* antitumor effect of E-[c(RGDfK)$_2$] and E-[c(RGDfK)$_2$]-paclitaxel in xenografted nu/nu mice (human ovarian carcinoma OVCAR-3) was evaluated. Although the half-life of E-[c(RGDfK)$_2$]-paclitaxel at physiological pH is limited, it could be sufficient for targeting to integrin $\alpha_v\beta_3$ considering that Janssen et al. determined the highest tumor/blood ratios of radiolabeled E-[c(RGDfK)$_2$] at 1–2 h post-injection (Janssen et al., 2002b) and Chen et al. confirmed this observation demonstrating the highest tumor uptake of radiolabeled E-[c(RGDyK)$_2$]-paclitaxel 2 h post-injection (Chen et al., 2005).

Very recently *in vivo* data of the related E-[c(RGDyK)$_2$]-paclitaxel in an orthotopic MDA-MB-435 breast cancer model were reported (Cao et al., 2008). The antitumor effect of the conjugate at a dose of 10 mg/kg paclitaxel equivalents in comparison to a combined therapy of paclitaxel and E-[c(RGDyK)$_2$] at doses of 10 mg/kg and 15 mg/kg was evaluated. Mice were treated i.p. every 3 days with a total of five doses. The conjugate showed an improved although moderate antitumor effect over paclitaxel but no tumor regression could be observed.

In an orientating *in vivo* experiment we compared E-[c(RGDfK)$_2$]-paclitaxel at a total dose of 3 × 12 mg/kg paclitaxel equivalents, paclitaxel at a total dose of 2 × 12 mg/kg and the free E-[c(RGDfK)$_2$] peptide at an equivalent dose in an OVCAR-3 model. Doses were administrated to mice i.v. in a weekly schedule. The results are summarized in Fig. 8 and Table 2. Although the overall doses are slightly lower than those in the experiment by Cao et al., our results do not confirm an improved efficacy of E-[c(RGDfK)$_2$]-paclitaxel derivative over free paclitaxel in the OVCAR-3 xenograft model. Paclitaxel showed moderate antitumor efficacy, but no efficacy was observed for E-[c(RGDfK)$_2$] or E-[c(RGDfK)$_2$]-paclitaxel (Fig. 8). Although the superior efficacy of paclitaxel was not statistically significant according to the criteria of $p < 0.05$ (*U*-test by Mann and Whitney) the differ-

Table 2
Dose schedule, mortality, body weight change, and antitumor activity of E-[c(RGDfK)$_2$]-paclitaxel, paclitaxel, and E-[c(RGDfK)$_2$] against human ovarian cancer xenografts (OVCAR-3) *in vivo*.

Substance	Nu/nu mice	Treatment (d)	Dose (mg/(kg inj.))	Toxic deaths (d)	BWC (%) d 10–17	Optimum T/C (%) (at day)
5% Glucose-P-Buffer	8	10,17,24			−2	
Paclitaxel	8	10,17	12	0	−1	47 [38]
E-[c(RGDfK)$_2$]-paclitaxel	8	10,17,24	12	0	−1	86 [27]
E-[c(RGDfK)$_2$]	6	10,17,24	54,5	0	0	80 [27]

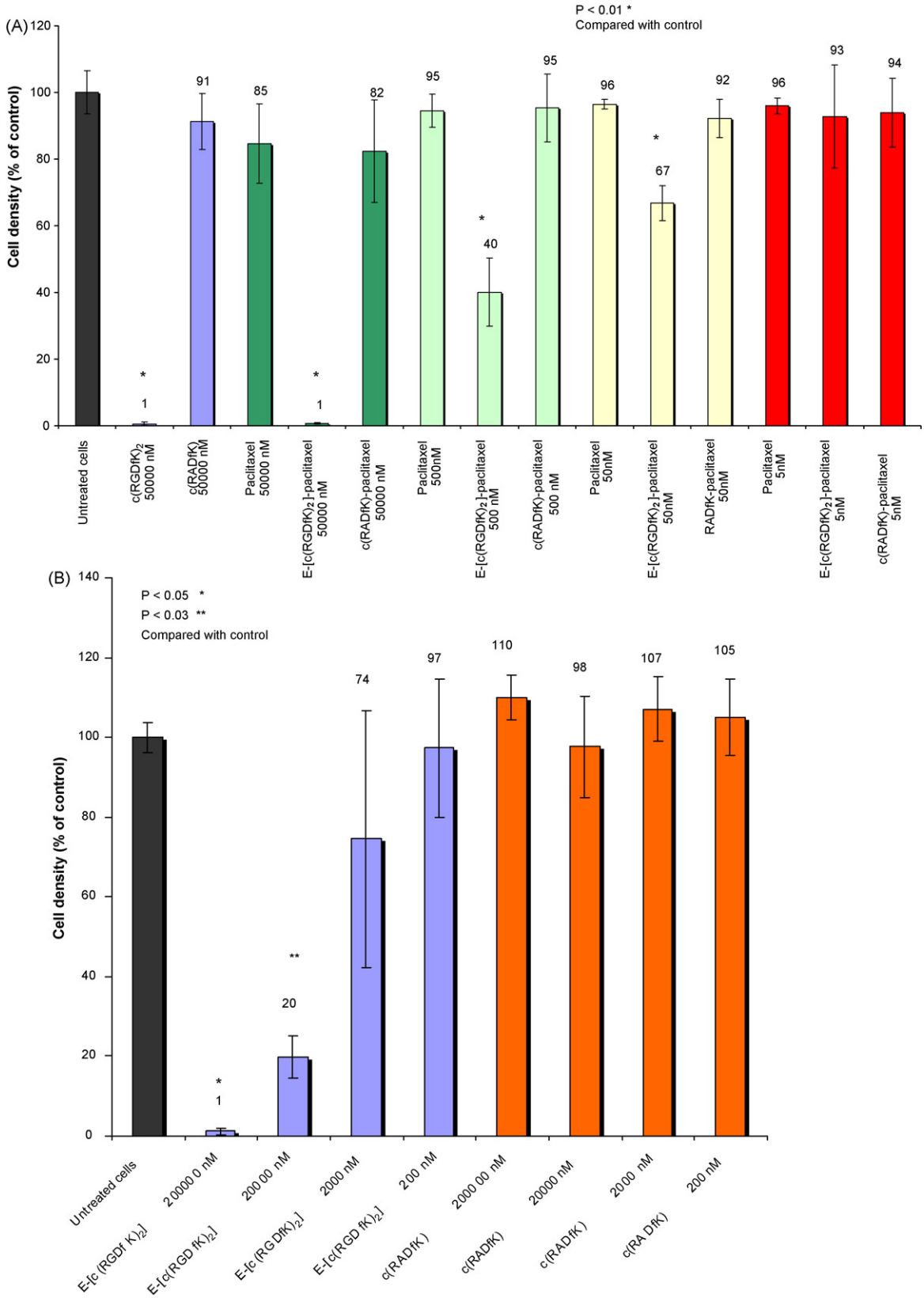

Fig. 7. (A) and (B) endothelial cell adhesion assay with paclitaxel, the paclitaxel derivatives and E-[c(RGDfK)$_2$] and c(RADfK). All concentrations are expressed as paclitaxel-equivalent concentrations.

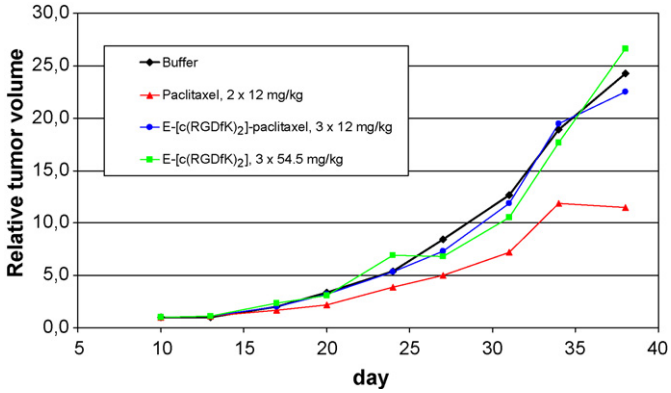

Fig. 8. Curves depicting tumor growth inhibition of subcutaneously OVCAR-3 xenografts under therapy with E-[c(RGDfK)$_2$]-paclitaxel, paclitaxel, and E-[c(RGDfK)$_2$].

ence between paclitaxel and E-[c(RGDfK)$_2$]-paclitaxel derivative is apparent.

There are a number of reasons that could explain the lack of efficacy of the paclitaxel RGD conjugate: (a) the targeting potential of E-[c(RGDfK)$_2$]-paclitaxel is insufficient per se although this explanation does not seem likely considering the convincing evidence of tumor uptake that Janssen et al. has collected with radiolabeled (RGDfK)$_2$ in the OVCAR-3 xenograft model, the same that model that we used in our studies (Janssen et al., 2002b); (b) hydrolysis of the ester bond at the 2′-OH position of paclitaxel leads to premature release of paclitaxel in the circulation with a concomitant decrease of paclitaxel reaching the tumor site; (c) the potency of paclitaxel is not sufficient for receptor targeting of integrin $\alpha_v\beta_3$. The interaction of E-[c(RGDfK)$_2$]-paclitaxel with integrin might be limited due to an insufficient receptor density on endothelial cells or a rapid clearance of E-[c(RGDfK)$_2$]-paclitaxel leading to low amounts of paclitaxel reaching endothelial cells. Thus, targeting of integrin $\alpha_v\beta_3$ expressing cells could be improved by using highly potent cytotoxic drugs in line with the clear trend of using such agents for the development of drug antibody conjugates that are designed for receptor or antigen targeting (Kratz et al., 2008; Wu and Senter, 2005).

In summary, the RGD paclitaxel conjugate (E-[c(RGDfK)$_2$]-paclitaxel) provided promising results *in vitro* but did not show any antitumor effect *in vivo*. As a conclusion, RGD drug conjugates with other drugs and/or more stable or other linkers should be investigated.

Acknowledgements

The support of the Mildred Scheel Stiftung der Deutschen Krebshilfe is gratefully acknowledged. This study was supported by a Postdoctoral Fellowship (HMS) from the Israel Cancer Research Fund. This work was partly supported by THE ISRAEL SCIENCE FOUNDATION (1300/06), a grant from the Alon Foundation, and the Israel Cancer Association to RSF.

References

Aumailley, M., Gurrath, M., Müller, G., Calvete, J., Timpl, R., Kessler, H., 1991. Arg-Gly-Asp constrained within cyclic pentapeptides. Strong and selective inhibitors of cell adhesion to vitronectin and laminin fragment P1. FEBS Lett. 291, 50–54.

Buerkle, M.A., Pahernik, S.A., Sutter, A., Jonczyk, A., Messmer, K., Dellian, M., 2002. Inhibition of the alpha-nu integrins with a cyclic RGD peptide impairs angiogenesis, growth and metastasis of solid tumours in vivo. Br. J. Cancer 86, 788–795.

Burkhart, D.J., Kalet, B.T., Coleman, M.P., Post, G.C., Koch, T.H., 2004. Doxorubicin–formaldehyde conjugates targeting $\alpha_v\beta_3$ integrin. Mol. Cancer Ther. 3, 1593–1604.

Cao, Q., Li, Z.B., Chen, K., Wu, Z., He, L., Neamati, N., Chen, X., 2008. Evaluation of biodistribution and anti-tumor effect of a dimeric RGD peptide-paclitaxel conjugate in mice with breast cancer. Eur. J. Nucl. Med. Mol. Imag., EPub.

Chen, X., Plasencia, C., Hou, Y., Neamati, N., 2005. Synthesis and biological evaluation of dimeric RGD peptide-paclitaxel conjugate as a model for integrin-targeted drug delivery. J. Med. Chem. 48, 1098–1106.

Dechantsreiter, M.A., Planker, E., Matha, B., Lohof, E., Holzemann, G., Jonczyk, A., Goodman, S.L., Kessler, H., 1999. *N*-Methylated cyclic RGD peptides as highly active and selective alpha(V)beta(3) integrin antagonists. J. Med. Chem. 42, 3033–3040.

Deutsch, H.M., Glinski, J.A., Hernandez, M., Haugwitz, R.D., Narayanan, V.L., Suffness, M., Zalkow, L.H., 1989. Synthesis of congeners and prodrugs. 3.1 Water-soluble prodrugs of taxol with potent antitumor activity. J. Med. Chem. 32, 788–792.

Dosio, F., Brusa, P., Crosasso, P., Arpicco, S., Cattel, L., 1997. Preparation, characterization and properties in vitro and in vivo of a paclitaxel-albumin conjugate. J. Control. Release 47, 293–304.

Friess, H., Langrehr, J.M., Oettle, H., Raedle, J., Niedergethmann, M., Dittrich, C., Hossfeld, D.K., Stöger, H., Neyns, B., Herzog, P., Piedbois, P., Dobrowolski, F., Scheithauer, W., Hawkins, R., Katz, F., Balcke, P., Vermorken, J., van Belle, S., Davidson, N., Esteve, A.A., Castellano, D., Kleeff, J., Tempia-Caliera, A.A., Kovar, A., Nippgen, J., 2006. A randomized multi-center phase II trial of the angiogenesis inhibitor Cilengitide (EMD 121974) and gemcitabine compared with gemcitabine alone in advanced unresectable pancreatic cancer. BMC Cancer 6, 285.

Haubner, H., Gratias, R., Diefenbach, B., Goodman, S.L., Jonczyk, A., Kessler, H., 1996. Structural and functional aspects of RGD-containing cyclic pentapeptides as highly potent and selective integrin $\alpha_v\beta_3$ antagonists. J. Am. Chem. Soc. 118, 7461–7472.

Janssen, M., Oyen, W.J., Massuger, L.F., Frielink, C., Dijkgraaf, I., Edwards, D.S., Radjopadhye, M., Corstens, F.H., Boerman, O.C., 2002a. Comparison of a monomeric and dimeric radiolabeled RGD-peptide for tumor targeting. Cancer Biother. Radiopharm. 17, 641–646.

Janssen, M.L., Oyen, W.J., Dijkgraaf, I., Massuger, L.F., Frielink, C., Edwards, D.S., Rajopadhye, M., Boonstra, H., Corstens, F.H., Boerman, O.C., 2002b. Tumor targeting with radiolabeled $\alpha_v\beta_3$ integrin binding peptides in a nude mouse model. Cancer Res. 62, 6146–6151.

Janssen, M., Frielink, C., Dijkgraaf, I., Oyen, W., Edwards, D.S., Liu, S., Rajopadhye, M., Massuger, L., Corstens, F., Boerman, O., 2004. Improved tumor targeting of radiolabeled RGD peptides using rapid dose fractionation. Cancer Biother. Radiopharm. 19, 399–404.

Kratz, F., Müller, I.A., Ryppa, C., Warnecke, A., 2008. Prodrug strategies in anticancer chemotherapy. ChemMedChem 3, 20–53.

Kussmann, M., Lässing, U., Stürmer, C.A., Przybylski, M., Roepstorff, P., 1997. Matrix-assisted laser desorption/ionization mass spectrometric peptide mapping of the neural cell adhesion protein neurolin purified by sodium dodecyl sulfate polyacrylamide gel electrophoresis or acidic precipitation. J. Mass Spectrom. 32, 483–493.

Luo, Y., Prestwich, G.D., 1999. Synthesis and selective cytotoxicity of a hyaluronic acid-antitumor bioconjugate. Bioconjugate Chem. 10, 755–763.

MacDonald, T.J., Taga, T., Shimada, H., Tabrizi, P., Zlokovic, B.V., Cheresh, D.A., Laug, W.E., 2001. Preferential susceptibility of brain tumors to the antiangiogenic effects of an alpha(v) integrin antagonist. Neurosurgery 48, 151–157.

Nabors, L.B., Mikkelsen, T., Rosenfeld, S.S., Hochberg, F., Akella, N.S., Fisher, J.D., Cloud, G.A., Zhang, Y., Carson, K., Wittemer, S.M., Colevas, A.D., Grossman, S.A., 2007. Phase I and correlative biology study of cilengitide in patients with recurrent malignant glioma. J. Clin. Oncol. 25, 1651–1657.

Pfaff, M., Tangemann, K., Müller, B., Gurrath, M., Müller, G., Kessler, H., Timpl, R., Engel, J., 1994. Selective recognition of cyclic RGD peptides of NMR defined conformation by $\alpha_{IIb}\beta_3$, $\alpha_v\beta_3$, and $\alpha_5\beta_1$ integrins. J. Biol. Chem. 269, 20233–20238.

Temming, K., Schiffelers, R.M., Molema, G., Kok, R.J., 2005. RGD-based strategies for selective delivery of therapeutics and imaging agents to the tumour vasculature. Drug Resist. Update 8, 381–402.

Tucker, G.C., 2006. Integrins: molecular targets in cancer therapy. Curr. Oncol. Rep. 8, 96–103.

Wu, A.W., Senter, P.D., 2005. Arming antibodies. Nat. Biotechnol. 23, 1137–1146.